



ELSEVIER

Nuclear Instruments and Methods in Physics Research B 157 (1999) 259–269

**NIM B**  
Beam Interactions  
with Materials & Atoms

www.elsevier.nl/locate/nimb

## Probing aqueous-organic interfaces with soft-landed ions

K. Wu<sup>a</sup>, M.J. Iedema<sup>a</sup>, A.A. Tsekouras<sup>b</sup>, J.P. Cowin<sup>a,\*</sup>

<sup>a</sup> *Environmental Molecular Sciences Laboratory, Pacific Northwest National Laboratory, Battelle Blvd., P.O. Box 999, MIS K8-88, Richland, WA 99352, USA*

<sup>b</sup> *Laboratory of Physical Chemistry, University of Athens, Athens GR-15771, Greece*

---

### Abstract

A very low energy ion source (1 eV) is used to dose hydronium ions on or into epitaxially grown amorphous thin films of water and organic solvent, from tens to thousands of monolayers thick. This is done to probe the structure of the organic film, ion diffusion and solvation, and the kinetics of transfer of hydronium ions from an aqueous environment into a non-aqueous one. The organic solvent used is methyl cyclohexane. Water dosed from 0 to 0.5 monolayer on top of 60 monolayer films of methyl cyclohexane causes a solvation of ions co-adsorbed with the water, slowing the subsequent diffusion of ions through the solvent film. Water in excess of a monolayer causes extreme slowing of ion transfer into the organic phase. Structures in the film, due to intentional doping or crystallization, are also probed via the ion motion. © 1999 Elsevier Science B.V. All rights reserved.

*PACS:* 68.15.+e; 51.50.+v; 72.20.i; 79.20.Rf

*Keywords:* Ions; Hydronium; Mobility; Solvation; Phase transfer

---

### 1. Introduction

Transport properties of ions through organic layers are central to topics as diverse as cell wall transport, fuel cells, chemical sensor electrodes, reactions and separations using non-aqueous solvents, organic electronics, photographic film, and food packaging. It is often difficult to measure ion mobility easily in organic materials, as it has been usually not possible to create systems where the

ion identity, transport distance, and times are all simultaneously well defined.

An ideal way to study these phenomena would be to recreate these ionic systems using molecular beam and ion beam technology. In this fashion we could hope to create systems where the identity, amount, and position of the ionic species might be tailored at the atomic scale, at least along the normal to the surface. We could recreate acceptor–donor pairs of ions to explore oxidation, explore diffusion over known distances, etc. To do this we need two things: (1) an ion beam that is gentle enough to deposit pure ions of chemical interest; (2) liquids that will ‘stay put’, that is not evaporate too quickly, nor allow ion or solvent diffusion until we want them to occur.

---

\* Corresponding author. Tel.: +1-509-376-6330; fax: +1-509-376-6066; e-mail: jp.cowin@pnl.gov

To accomplish the latter, we employ cryogenic, vapor-deposited amorphous films of solvents we wish to study. Many organic solvents upon vapor deposition at cryogenic temperatures form amorphous deposits with liquid-like structure. Upon warming above their glass temperatures, these become true liquids, whose transport kinetics can be altered from nearly infinitely slow to quite fast by simply adjusting the temperature. The vapor pressures can also be conveniently low, permitting use of vacuum-based instrumentation, and for films initially thousands of monolayers thick, time to explore their properties up to temperatures where their vapor pressure is around  $10^{-3}$  Torr. We have, for example, explored n-hexane and 3-methylpentane films up to about 150 K, providing a wide useful range above their glass temperature which is near 80 K [1]. In this study we report on results using methyl cyclohexane (MCH), which has a glass temperature of 85 K [2,3], and can be studied up to around 150 K.

Water also deposits as an amorphous film. We can explore its liquid-like properties from its glass temperature of about 135 K through its crystallization temperature of around 165 K, and transport properties of the crystalline ice to about 200 K [4], where its vapor pressure becomes too high. Surprisingly to us, we found no ion motion (either of  $\text{Cs}^+$  or of hydronium) in either amorphous ice [5] above its glass temperature or in crystalline ice [4]. This means that many studies we envisioned doing to study ion motion in water would not be possible!

This study reports on our attempts to usefully probe ion transport away from the water-organic interface. This should not be prevented from happening by water ices' inability to transport ions.

Separation processes for ionic species, like  $\text{Cs}^+$ , from complex mixtures (such as Hanford tank waste), or in biological transfer of ions across membranes, involve moving an ion from a well-solvated aqueous region into an organic medium with poorer solvation [6–8]. We have begun studies of this using a soft-landed ion source. We introduce ions on top of an organic layer, and then look at the ability of small amounts of added water to inhibit the motion of the ion. The water is expected

to alter the motion in two ways: At sub-monolayer amounts of water, illustrated in Fig. 1a, we anticipate that the water molecules will form a water-ion complex. This will increase the size of the ion, and will thus slow down the ion by increasing its viscous drag. We should then expect to measure via the amount it has slowed the hydration state of the ion. The hydration number of the ion ought to vary with the amount of water deposited and the thermal history. For thicker water films the ion becomes fully hydrated in the water film. We expect the energy of the ion to be lowest if it remains in the aqueous layer, and we should see much greater inhibition of the ion motion. This is shown in Fig. 1b.

We have a newly developed soft-landed ion source that is very effective for these studies [9]. Soft-landed ions are a powerful new tool, now being exploited by a handful of researchers [10,11] to probe a variety of interfacial problems. As described in Section 2, it provides 1 eV ions at several nanoamps, which land without collision-induced damage to either the ions or the substrate. The 1 eV energy of our beam is lower than that of other soft-landing ion sources [10,11], i.e., we can work without cushioning layers and are not limited to very robust ions.

## 2. Experimental

The experiments were performed in an ultra-high vacuum apparatus [5,9] designed for surface science studies. It has a base pressure of  $2 \times 10^{-10}$  Torr.

The crystal could be positioned in front of any of the following instruments located on the walls of the chamber. A molecular beam source was used to deposit known amounts of methyl cyclohexane (MCH) vapor (from repetitively freeze-thaw-degassed liquids). A typical beam flux on the crystal was 1 monolayer per 7 s. An Auger spectrometer was used to inspect surface cleanliness. A sputter gun was used occasionally if persistent carbon, calcium, or indium was detected at or above a one percent level. A computer-driven quadrupole mass spectrometer with electron im-

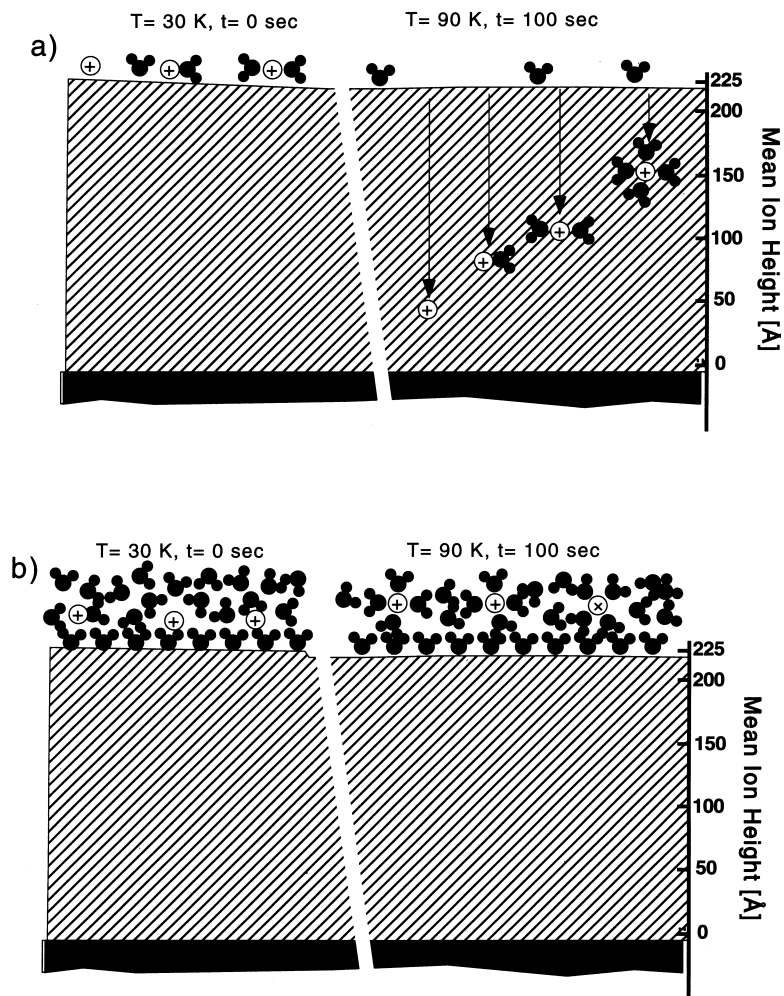


Fig. 1. *Phase transfer of ions*: Shown are scenarios for hydration effects at the interface of organic film regarding transfer of an ion into the medium. The organic film is shaded, co-adsorbed water molecules are in black, the Pt(111) substrate is at the bottom of the film. (a) shows size effect of hydration on mobility, (b) indicates that for large amounts of co-adsorbed water, a true aqueous phase exists, which will stabilize the ion, preventing motion into the organic film.

pact ionization (UTI) monitored the amounts of gases desorbing from the crystal.

The ion source [5,9] consisted of several differentially pumped stages with ion optics that ensured beam uniformity, low energy spread, low neutral load, and ion selectivity. Ions from the nozzle region were accelerated to 300 eV to travel the majority of the length of the beam, finally to be decelerated just in front of the crystal in a short, planar decelerator consisting of a double-mesh and the crystal. The final energy when reaching the

crystal was near 1 eV.  $\text{D}_3\text{O}^+$  ions were created by collisions of 150 eV electrons in the expansion region of a pure  $\text{D}_2\text{O}$  beam, creating  $\text{D}_2\text{O}^+$ . The latter ion then collided with either neutral water molecules in the expanding molecular beam or the steady-state chamber background, to form  $\text{D}_3\text{O}^+$  and DO. We currently place a short tube in front of the nozzle with a side slit to let electrons through, to enhance hydronium production, and to stabilize electron emission from the filament by lowering the pressure it sees. The  $\text{D}_3\text{O}^+$  was

separated from other ionic species present using a Colutron Wien filter.

Charging of the crystal surface and work function changes were measured using an oscillating, gold-plated electrode (Kelvin Probe 6000, McAllister Technical Services) equipped with digital and analog output. A few millivolts precision was achieved.

It is particularly important that the ion beam, which will deposit on the order of 0.001 monolayers of ions over 1–30 min, does not simultaneously contaminate the surface with water vapor. The differential pumping and two ion beam bends alone allow deposition of about 0.25 monolayer of water during typical ion deposition, which is not acceptable. This amount is reduced to a negligible level of 1% of a monolayer of water co-adsorbed through the use of two cryotrap cooled by liquid nitrogen, one in the ion source and another in front of the crystal.

A typical experiment was performed in three stages (see Fig. 2). First, a layer of solvent was vapor-deposited on the surface of a clean Pt(1 1 1) crystal. Water would be adsorbed, when desired, before or after the ions were added. Then, an ion beam with energy below 1.2 eV and currents up to 2 nA was aimed at the crystal at normal incidence, creating a layer of ions on top of the molecular

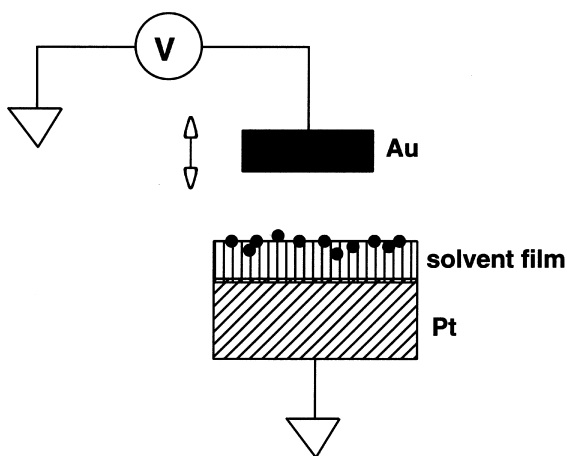


Fig. 2. *Experimental procedure:* After ions are deposited on film, their position is monitored via a non-contacting vibrating gold foil (Kelvin probe), which measures the work function changes of the system.

adsorbate. During this deposition of ions, the film would charge like a capacitor. This charging could be monitored by quickly sweeping the crystal bias through several volts and recording the ion beam current, generating a ‘stopping curve’. Shifts of this curve indicated charging, which then required readjusting the crystal bias to maintain the ion impact energy near 1 eV. The final measurement consisted of simultaneously monitoring adsorbate partial pressure in the gas phase and crystal work function while ramping the temperature.

Sticking probabilities are near unity. Coverages for MCH and water are reported in multiples of that which saturates the most strongly bound state on the surface, judged by thermal desorption. For water 1 monolayer (ML) is  $1.05 \times 10^{15} \text{ cm}^{-2}$ , and for MCH, it is assumed that it is the same as for n-hexane:  $2.1 \times 10^{14} \text{ cm}^{-2}$  (or  $48 \text{ \AA}^2/\text{molecule}$ ) [13,1].

The ions on the dielectric ices create a capacitor and alter the external work function by

$$\Delta\phi = \frac{-QL}{A\epsilon\epsilon_0} \equiv -\Delta V_{\text{film}}, \quad (1)$$

where  $Q$  is the charge deposited,  $A$  the area,  $L$  the film thickness,  $\epsilon$  the film permittivity (dielectric constant),  $\epsilon_0$  the vacuum permittivity, and  $\Delta V_{\text{film}}$  we define as the ‘film voltage’. When  $\epsilon$  is constant, as it nearly is for MCH, the motion of the ions can be tracked by changes in the work function. Motion of the ions into the film will create within the ice film a charge distribution. It can be shown [1] that at any moment Eq. (1) gives us the mean ion height  $\langle z \rangle$  above the surface, if we replace  $L$  with  $\langle z \rangle$ . That is, the 3-D ion distribution function  $\rho(x, y, z)$  contributes to the macroscopic film voltage only through the integral of  $z$  times  $\rho(x, y, z)$ , giving  $\langle z \rangle$ .

### 3. Results

#### 3.1. Thermal desorption data

Fig. 3 shows thermal desorption data for MCH for coverages from 0.89 to 5.3 monolayers. For the previous work on adsorption of MCH on Pt(1 1 1) see Ref. [12] (and note dehydrogenation channel). Note that the desorption peak at 238 K is much

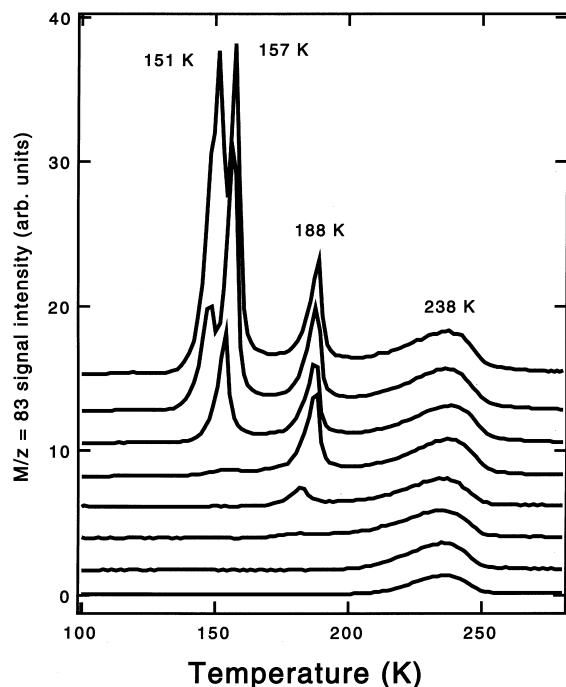


Fig. 3. *Temperature programmed desorption spectra*: Temperature programmed desorption spectra are shown for 0.89, 1.0, 1.1, 1.4, 2.0, 2.7, 4.0, and 5.3 monolayers of adsorbed methyl cyclohexane (MCH). MCH was adsorbed at 30–50 K, then the substrate was heated at 3 K/s. Desorption is monitored through the most abundant ion fragment of MCH, i.e.,  $C_6H_{11}^+$  which has  $m/z = 83$ .

higher than the other peaks: typical for most hydrocarbons adsorbed on metals [13,1]. The thermal desorption data, with several distinct peaks at lower binding energy indicate some complex packing onto the surface. Beyond the coverages shown here, the low temperature peak simply grows, subsuming the other features, and is a typical zero-order desorption peak corresponding to bulk evaporation of MCH. From this we see that a thick film should stay in place to around 150 K (higher coverages move this desorption slightly upward in  $T$ , but the slower heating rate used while measuring ion diffusion brings it back down slightly).

Water desorbs at low coverage from the clean Pt surface at around 175 K, and for multilayer water, around 160 K.

### 3.2. Basic results: no water

Fig. 4 shows the evolution of the contact potential difference (equal to the film voltage in Eq. (1)) for ions dosed on top of MCH, for several initial thicknesses. The curves have almost the same electric field strength, except for the thickest, which is somewhat weaker. In each case as the temperature is ramped upward, the film voltage at first remains nearly constant, then begins to reduce gradually starting at around 40–60 K, and finally drops rapidly to near zero just below 100 K. This voltage drop directly reflects the mean ion position in the film.

The ions move through the film because they are in an attractive electric field that they collectively generate. Each ion effectively sees in the metal substrate a negative image of itself and all its neighbors and is attracted towards it. Ion motion over distances  $L$  in the presence of an electric field  $E$ , such that  $L|E|$  is much greater than  $kT$ , is

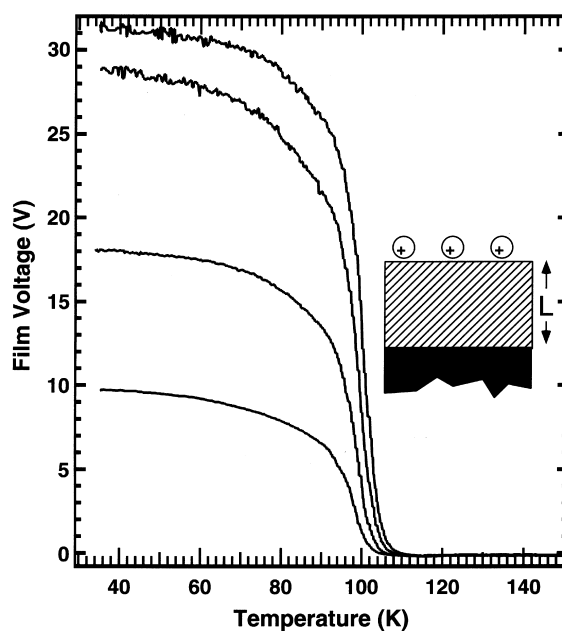


Fig. 4. *Ion motion at several MCH thicknesses*: Shown is the film voltage drop due to hydronium ion motion into MCH films, as the temperature is ramped, for initial coverages of 30, 60, 90, 120 ML, from bottom to top. Films grown near 30 K, ion dosed at 30 K, then the temperature was ramped at 0.2 K/s.

dominated by the drift velocity imparted by the field. Up to fairly large fields this drift velocity is linear with the field, and the proportionality factor is the ion mobility  $\mu$ . This mobility is a strong function of the viscosity of the material. The well-known Stokes–Einstein equation for the mobility of an ion of charge  $nq_e$  is based on the formula for the viscous drag on a macroscopic sphere of radius  $r_{\text{ion}}$  moving in a fluid of viscosity  $\eta$ , and is

$$\mu(T) = \frac{nq_e}{6\pi r_{\text{ion}}\eta(T)}. \quad (2)$$

The Stokes equation is not expected to be highly accurate, but typically gives estimates within a factor of several folds of experimentally measured mobilities [14]. We use this relation to analyze our data.

Integration of the field-induced motion effects on an initially thin layer of ions on a diffusive medium can be done nearly in closed form [1]. Any initially narrow distribution can be easily shown to quickly become a square distribution. The temporal dependence of the corresponding voltage changes form when the leading edge of the distribution reaches the bottom of the film, i.e., when  $V_{\text{film}} = V_0/2$ . The voltage versus time thus has different functional forms before and after this moment:

$$V_{\text{film}}(t) = V_0 \left[ L - t \frac{V_0}{2L} \bar{\mu}(t) \right] \frac{1}{L} \quad \text{for } V_{\text{film}} \geq \frac{V_0}{2}, \quad (3a)$$

$$V_{\text{film}}(t) = \frac{L^2}{2t\bar{\mu}(t)} \quad \text{for } V_{\text{film}} < \frac{V_0}{2} \quad (3b)$$

with

$$\begin{aligned} \bar{\mu}(t) &\equiv \frac{1}{t} \int_0^t dt' \mu(T(t')) \\ &\approx \frac{nq_e}{6\pi r} \frac{1}{t} \int_0^t dt' \frac{1}{\eta(T(t))}. \end{aligned} \quad (3c)$$

Methyl cyclohexane's viscosity has not been as extensively measured at very low temperatures compared to some glasses like 3-methylpentane [15]. This is especially true when pure, largely as it has some tendency to crystallize. Carpenter et al.

[2] give data points from about 137 to 310 K. To extrapolate to the temperatures where the ions are seen to move in MCH, we use the Vogel–Tamman–Fucher equation for the viscosity,  $\eta(t) = A \exp(E_a/(R(T - T_0)))$  [3]. Since it is a long extrapolation for the MCH data, we added a point to the data in Fig. 5, one at  $10^{12} \text{ kg m}^{-1} \text{ s}^{-1}$  at MCH's calorimetric glass transition temperature of 85 K. This is a common definition of the glass temperature, and is often fairly accurate at (or extrapolated to) the calorimetric glass temperature [3]. The fitted parameters are in Table 1.

Before numerically simulating the data in Fig. 4, we can qualitatively compare them against themselves. First, regardless of whether the ion motion is inversely proportional to the viscosity, the curves of Fig. 4 should have the same shape at low temperatures. That is, an ion would have no way to know the thickness of the film if the field

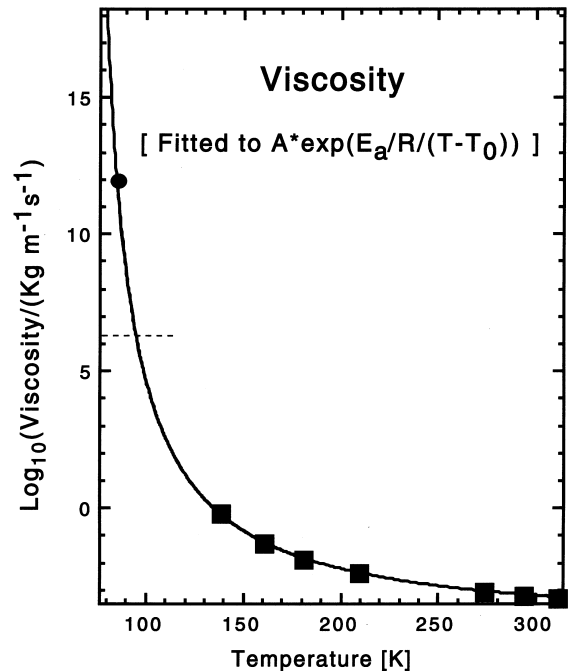


Fig. 5. *MCH* viscosities: The experimental data (squares) from Ref. [2] are shown for methyl cyclohexane. Also shown is a fit to the data using a Vogel–Tamman–Fucher equation. The point (filled circle) at  $10^{12} \text{ kg m}^{-1} \text{ s}^{-1}$  is estimated using the known calorimetric glass temperature. The dashed curve is roughly that needed to fit our measured results in Fig. 7.

Table 1  
Viscosity fitting parameters

A	$2.87 \times 10^{-5} \text{ kg m}^{-1} \text{ s}^{-1}$
$E_a$	$5960 \text{ kJ mole}^{-1}$
$T_0$	66.2 K

strength is constant, until some ions actually reach the bottom of the film. This should be true if Eqs. (3a)–(3c) are correct until ions first hit bottom, at the 1/2 point in the voltage decay. In Fig. 6a we show all four curves offset to start together. We see that the curves deviate from each other already by 60 K, and when the thinnest film is much before the 1/2 point. Contrary to a simple model, some ions move all the way through the film even by 60 K. Eq. (3b) shows that independent of the initial voltage, for simple mobility-determined motion,

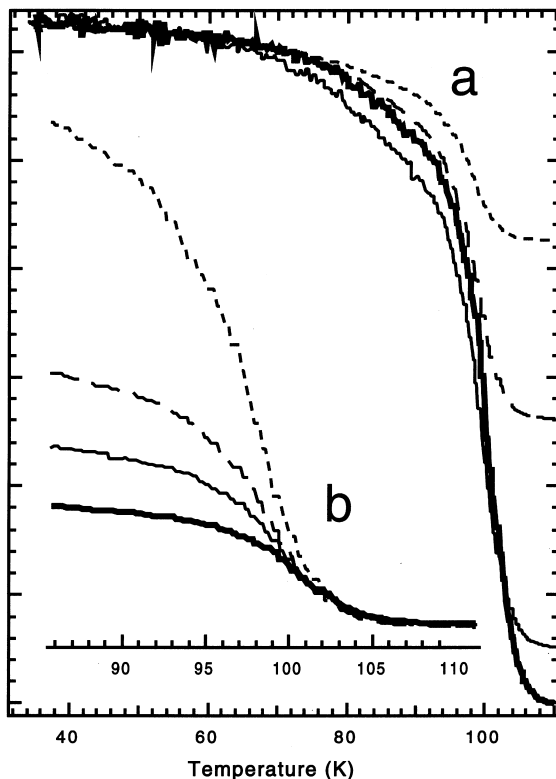


Fig. 6. Comparing curves: The data from Fig. 4 are compared against themselves (see text). The short dashed curves are for 30 ml MCH, and the long dash, solid, and thick solid lines are for 60, 90, and 120 ML, respectively.

curves re-scaled by  $1/L^2$  should all match after the 1/2 point. Appropriately re-scaled curves are shown in Fig. 6b. This time, the curves do all match closely, though only for the last 1/4 or so rather than 1/2 of the curves. Perhaps only at the lower fields is Eqs. (3a)–(3c) valid.

Using the published viscosity, and  $r_{\text{ion}}$  set to 3 Å, we calculate the set of dashed curves in Fig. 7. Very broadly the agreement with the experimental is only partial: we predict within a few degrees the gross fall off near 100 K. But the experimental fall off for each curve spans about 2–3 times wider a temperature range than theory predicts. And the shift with coverage is about twice as strong as theory predicts. Also, very unlike the theory, the experimental voltage falls considerably at low temperature, even well below the glass temperature of 85 K.

The most likely reason we agree poorly with the theory is that our field strength is too high for a simple mobility to be valid. To test this we did studies at progressively lower fields, for a constant thickness film as shown in Fig. 8. As the field is

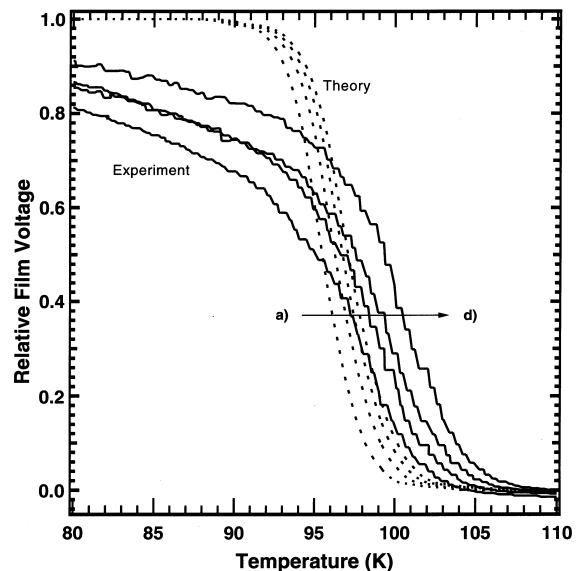


Fig. 7. Comparing theory and experiment: The data from Fig. 4 (solid lines) expanded near 100 K are compared against theory (dashed lines) as explained in the text (a) 60 ML, (b) 120 ML, (c) 180 ML, (d) 240 ML.

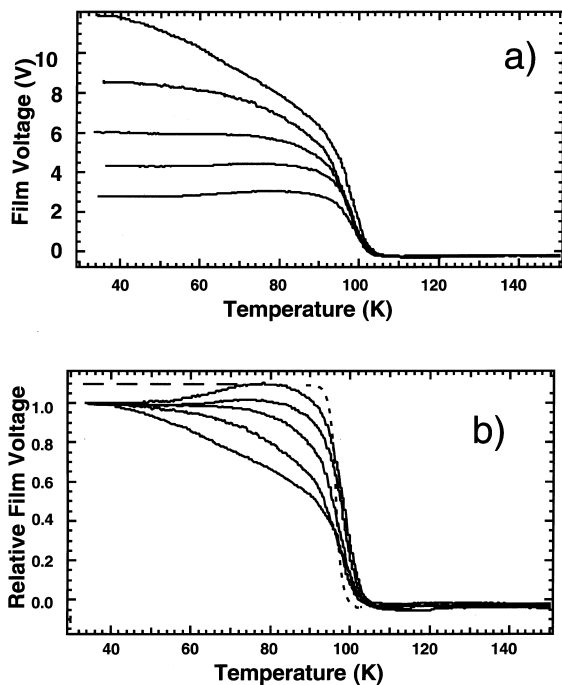


Fig. 8. *Field effects*: 30 ML films of MCH, at increasing field strength: (a) from bottom to top 2.72, 4.40, 5.86, 8.50,  $11.7 \times 10^8$  V/m (assuming 3.41 Å per nominal monolayer); (b) re-scaled from (a). The top curve in (b) is for the weakest field. The long dashed line in panel (b) is after correcting for the ferroelectric effect in the thickest films; the short dashed curve is from theory.

lowered, the curves lose the fall off below the glass temperature. And the rapid fall near 100 K sharpens considerably at lower fields. Fig. 8b shows the theory results using Eqs. (2)–(3c). The fit is better than for the higher field cases. Note that the experimental curves at the lower initial field actually curve upward as the temperature is ramped upward. This is due to a ferroelectric effect [16]. MCH lacks a center of symmetry, hence should possess a small molecular dipole, perhaps about 0.1 Debye. Asymmetric molecules, when vapor deposited at very low temperatures, tend to develop a slight net alignment in the growing film, putting some net dipole outward on the average for each molecule. This creates a net work function change per monolayer deposited, which is about 10 mV/ML for MCH. This disappears upon slight annealing in MCH by 80 K, and accounts quantitatively for the upward shift in the lowest field data in Fig. 8.

Studies using more conventional means [17,18] of measuring ion mobility have in general claimed that ion mobilities often strongly increase when the field strength exceeds  $10^7$  V/m. Our highest fields were 40 times this limit. To appreciate some reasons for the higher mobility, consider: The field dependence of the ion motion, particularly at temperatures below the glass temperature, might be attributable to an individual ion locally applying so much force, that the yield stress of the glass is exceeded. A singly charged ion in a field of  $4 \times 10^8$  V/m experiences a force of  $4.8 \times 10^{-11}$  N. This force, if assumed to be spread over the area of a single solvent molecule ( $6 \times 6$  Å) creates a pressure or shear/compression stress of  $1.3 \times 10^8$  Pa = 1300 atmosphere, or 20 000 lbs/in<sup>2</sup>. This is around the tensile stress of aluminum at room temperature. The force is also around 0.04 eV/Å, which over the width of a molecule greatly exceeds  $kT$ . It is also comparable to the van der Waals forces holding one molecule against the next.

Another way ions can move at high fields can be appreciated if one notes that the energy released by the ion as it traverses a single molecule is about  $q_e \times 4 \times 10^8$  V/m  $\times 6 \times 10^{-10}$  m or 0.24 eV. Now at 50 K, the internal modes of a hydrocarbon are largely frozen out. So the temperature rise a single molecule experiences will be limited by the heat capacity primarily of translational modes of the molecule as a whole, and similarly rotational degrees of freedom. The rise for this 6 R heat capacity would be about 500 K. If it holds on to this for 10 ps or so, this will greatly facilitate moving the ion past the next molecule. This is also made more plausible by realizing that this much energy is nearly enough to strip one molecule from the bulk and hurl it into the vacuum (that is, this is near the heat of vaporization ( $35.4$  kJ mole<sup>-1</sup>) of methyl cyclohexane [19]).

We can reduce the forces and stay within the linear mobility, and perhaps the Stokes law. This may be the best approach when one wants to use this as a tool to probe an unknown structure of an ion or medium. But fields of order  $4 \times 10^8$  V/m are extremely important in chemistry. This equals the force between two singly charged ions at a separation of 16 Å when immersed in a medium of dielectric constant of 2. So we might expect from

our results that two oppositely charged ions at 16 Å of each other could move through a typical organic solvent much faster than predicted by the Stokes equation, by exceeding the shear strength of the material. Even for a true liquid, where the zero frequency shear strength is zero, a yield stress is definable for rapidly applied forces (such as breaking taffy when pulled quickly).

### 3.3. Probing structures

Two examples are presented on probing structures. MCH, while considered a glass-forming material, has a tendency to crystallize when annealed. Crystalline MCH is not expected [1] to show significant ion diffusion, since it is not a liquid and has basically infinite viscosity. We can observe this via its blocking effect on ion motion. In Fig. 9 we present data for progressively more annealed MCH films (annealed either by growing

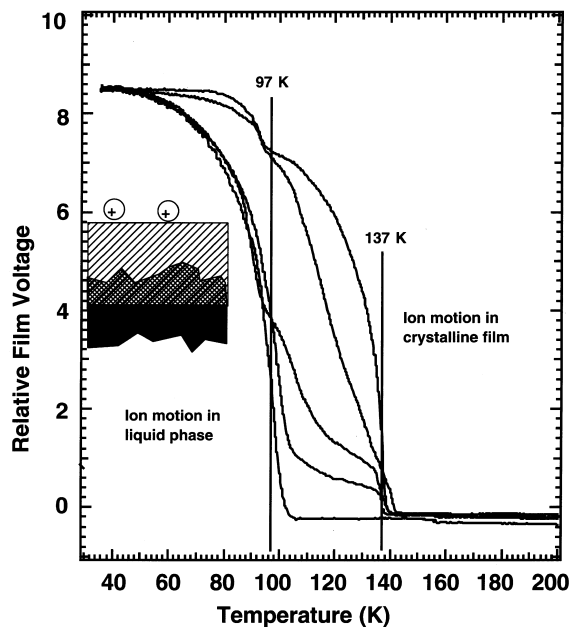


Fig. 9. *Probing crystallization*: The ion motion is altered by the crystallization of the film when it is annealed. Curves from left to right had the following recipes: 60 ML MCH grown at 30 K; 100 ML grown at 110 K; 110 ML MCH grown at 120 K; 210 ML MCH grown at 30 K then annealed by ramping at 0.2 K/s to 137 K and then dropped to 30 K; 210 ML MCH grown at 30 K then annealed via a ramp to 139 K and then dropped to 30 K.

them at low temperature, then heating briefly to a higher temperature, or else by vapor-depositing the film at a higher temperature). We see that for annealed films, the ions do not go all the way through. It would appear that annealing produces crystallization that propagates upward from the Pt(111) surface. The ions move downward and stop (at least till 137 K) at the crystalline boundary, as reflected in the voltage drop. Annealing to 139 K nearly completely crystallizes the film.

A second structure probing experiment is shown in Fig. 10. Here we created a synthetic structure: we imbedded 4 monolayers of water in between two 50 monolayer films of MCH. Ion motion now is in three steps: First the ions move through the top part of the film, just as in the simpler systems in Figs. 3 or 8. But then the ions reach the water layer and stop. At about 106 K, the ions resume moving through the film. Water molecules (or even a more subtly different doped layer, like benzene) have little chance to randomly move and disperse *before* the ions pass through, as neutral diffusion should be slower by factors

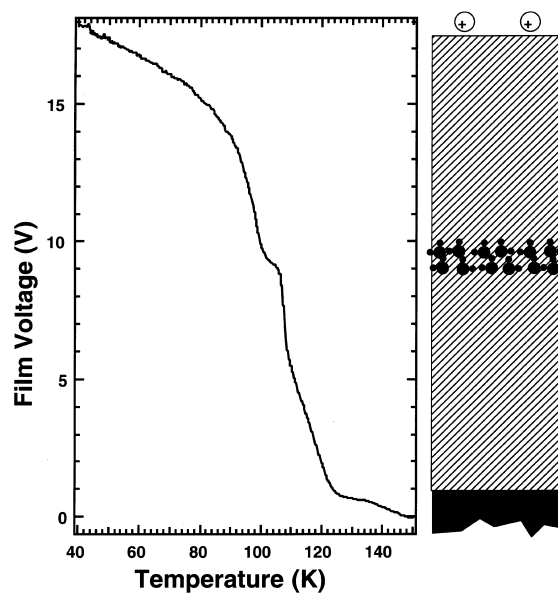


Fig. 10. *Probing internal structure*: A film was grown at 30 K with 50 ML of MCH on the bottom, then 4 ml of water, and then 50 ML of MCH. After deposition of hydronium ions, the temperature was ramped at 0.2 K/s.

roughly of the voltage difference across the film compared to  $kT$  [1]. (The ions certainly could disrupt the inside layer because of their passage, however.) So the transport or charge transfer properties of quite elaborately tailored liquids could be explored this way.

### 3.4. Adding water

Fig. 11 shows data for 60 ML films of MCH, upon which is placed water in increasing amounts, followed by hydronium ions. (We checked what difference it made putting the ions on top of or under the thin water film, and found none, contrary to what we might have expected based on the lack of hydronium mobility in thick water films [4].) As the samples were ramped in temperature, we see strong effects due to the water. First, the low temperature ion motion seen at these high fields disappears by the time 1 ml of water has been added. Also the rapid fall off at near 100 K is shifted upward in temperature. Finally, the curves develop a tail extending to 120 K. To plot the temperature shift versus water added, we face a choice due to changes in curve shape. We initially used the maximum slope temperature. But for the water-free curves this occurs near the end of the fall, while with water this occurs before the half-fall point. An alternative is to choose the temperature of the half height of the curve.

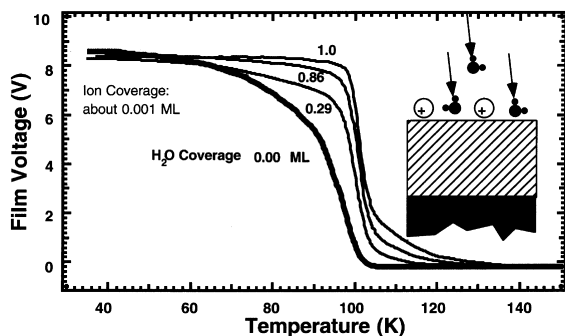


Fig. 11. *Hydrated ions on an organic film*: A film was first grown at 30 K with 60 ML of MCH (on the bottom). Water was then added to the coverages indicated. Next, ions were added at 30 K. Subsequently the temperature was ramped at 0.2 K/s.

Both analyses suggest the existence of a plateau between about 0.5 and 1 ML of added water, of 3 or 7.5 K. When more than 1 ML of water is added, a very large shift occurs which is too large to be accounted for by any change in mobility due to a simple increase in size. The plateau may be due to such a shift. However, at the fields used to date, the earlier discussion prohibits quantitative use of the Stokes equation to estimate the degree of hydration. Just the same, it may be that the plateau would suggest a large hydration shell of many waters. Titration experiments may explore the hydration number directly.

We are at present pursuing isothermal ion diffusion studies, with and without water. Those are much more sensitive to subtle changes such as hydration sphere size than these ramped experiments. The latter cover a huge dynamic range, and are precise to about 0.1 K.

We do see quite interesting effects due to changing MCH film thicknesses, which suggest a roughening of the film.

## 4. Conclusions

We have in these studies gone beyond just demonstrating that we have the ability to soft-land ions on surfaces. We have vigorously used it as a tool to probe ion motion in structured films, and have also shown that we can probe how strongly water impedes the motion of an ion into an organic film. Future experiments will fill the obvious need to use much lower fields to reach constant mobilities, making ion size measurements practical. But we also need to explore the high field motions, which are important to ion–ion reactions in organic solvents and in sensors, electrochemical cells, etc. We also plan to explore biological-type films regarding ion transport.

## Acknowledgements

Supported by Offices of Chemical Sciences of the Basic Energy Sciences Division of the Department of Energy. The Environmental Molecular Sciences Laboratory is supported by the DOE

Office of Biological and Environmental Research. Pacific Northwest National Laboratory is a multi-program national laboratory operated by Battelle Memorial Institute for the Department of Energy.

## References

- [1] A.A. Tsekouras, M.J. Iedema, J.P. Cowin, *J. Phys. Chem.* (submitted).
- [2] M.R. Carpenter, D.B. Davies, A.J. Matheson, *J. Chem. Phys.* 46 (1967) 2452.
- [3] C.A. Angell, *Science* 267 (1995) 1924.
- [4] J.P. Cowin, A.A. Tsekouras, M.J. Iedema, K. Wu, G.B. Ellison, *Nature* 398 (1999) 405.
- [5] A.A. Tsekouras, M.J. Iedema, G.B. Ellison, J.P. Cowin, *Internat. J. Mass Spect. Ion Processes* 174 (1998) 219.
- [6] N. Muzet, E. Engler, G. Wipff, *J. Phys. Chem. B* 102 (1998) 10772.
- [7] T.M. Chang, L.X. Dang, *J. Phys. Chem. B* 101 (1997) 10518.
- [8] I. Benjamin, *Chem. Rev.* 965 (1996) 1449.
- [9] J.P. Biesecker, G.B. Ellison, H. Wang, M.J. Iedema, A.A. Tsekouras, J.P. Cowin, *Rev. Sci. Instrum.* 69 (1998) 485.
- [10] A.W. Kleyn, *Science* 275 (1997) 1440.
- [11] S.A. Miller, H. Luo, S.J. Pachuta, R.G. Cooks, *Science* 275 (1997) 1447.
- [12] C. Xu, B.E. Koel, M.A. Newton, N.A. Frei, C.T. Campbell, *J. Phys. Chem.* 72 (1995) 16670.
- [13] L.E. Firment, G.A. Somorjai, *J. Chem. Phys.* 66 (1977) 2901.
- [14] G.J. Janz, R.P.T. Tomkins, *Non-Aqueous Electrolyte Handbook*, vol. 1, 1972, Academic Press, New York.
- [15] A.C. Ling, J.E. Willard, *J. Phys. Chem.* 72 (1968) 1918.
- [16] M.J. Iedema, M.J. Dresser, D.L. Doering, J.B. Rowland, W.P. Hess, A.A. Tsekouras, J.P. Cowin, *J. Phys. Chem.* 102 (1998) 9203.
- [17] A. Ioannidis, J.P. Dodelet, *J. Phys. Chem. B* 101 (1997) 891.
- [18] A. Ioannidis, J.P. Dodelet, in: R. Coelho (Ed.), *Physics of Dielectrics for the Engineer*, Elsevier, Amsterdam, 1979, p 124.
- [19] R. Fuchs, L.A. Peacock, *Canad. J. Chem.* 56 (1978) 2493.